White Rose Research Online

eprints@whiterose.ac.uk
https://eprints.whiterose.ac.uk
Universities of Leeds, Sheffield and York

Deposited via The University of York.

White Rose Research Online URL for this paper:
https://eprints.whiterose.ac.uk/id/eprint/239901/

Version: Published Version

Article:
Woodford, Timothy G., Male, Joshua S., Reardon, Christopher P. et al. (2026) On the practical utility of nanoimprint lithography for a small research laboratory. Nanotechnology. 105301. ISSN: 1361-6528

https://doi.org/10.1088/1361-6528/ae4c97

Reuse
This article is distributed under the terms of the Creative Commons Attribution (CC BY) licence. This licence allows you to distribute, remix, tweak, and build upon the work, even commercially, as long as you credit the authors for the original work. More information and the full terms of the licence here:
https://creativecommons.org/licenses/

Takedown
If you consider content in White Rose Research Online to be in breach of UK law, please notify us by emailing eprints@whiterose.ac.uk including the URL of the record and the reason for the withdrawal request.

UNIVERSITY OF LEEDS
University of Sheffield
UNIVERSITY of York

PURPOSE-LED PUBLISHING™

PAPER • **OPEN ACCESS**

On the practical utility of nanoimprint lithography for a small research laboratory

To cite this article: Timothy G Woodford *et al* 2026 *Nanotechnology* **37** 105301

View the article online for updates and enhancements.

You may also like

- Micro- and nano- patterning using imprinting technique
Haijing Lu, X C Shan, Yaofeng Sun et al.
- Nanoimprint Lithography on curved surfaces prepared by fused deposition modelling
Thomas Köpplmayr, Lukas Häusler, Iris Bergmair et al.
- Review of nanoimprinted photonics
Pei-Hsun Wang and Chih-Ming Wang

This content was downloaded from IP address 144.32.240.146 on 09/04/2026 at 12:29

Nanotechnology

Check for updates

OPEN ACCESS

RECEIVED
5 December 2025

REVISED
21 January 2026

ACCEPTED FOR PUBLICATION
3 March 2026

PUBLISHED
12 March 2026

Original content from this work may be used under the terms of the Creative Commons Attribution 4.0 licence.

Any further distribution of this work must maintain attribution to the author(s) and the title of the work, journal citation and DOI.

PAPER

On the practical utility of nanoimprint lithography for a small research laboratory

Timothy G Woodford[1,*], **Joshua S Male**[1], **Christopher P Reardon**[1] **and Thomas F Krauss**[1]

Photonics Group, School of Physics, Engineering and Technology, University of York, York, United Kingdom.
* Author to whom any correspondence should be addressed.

E-mail: timothy.woodford@york.ac.uk

Keywords: nanofabrication, imprint lithography, resin-stamp, electron-beam lithography, nanotechnologies, nanostructures, resonant photonics

Abstract

Nanoimprint lithography is a technique that promises a low-cost, high-throughput, and high-resolution method for fabricating nanostructures, which may be used in communications, sensing, and emerging technologies such as augmented reality glasses. We present a comprehensive analysis of an ultraviolet nanoimprint lithography protocol using a resin-stamp platform, introduced by OpTool AB, for the production of 1D and 2D guided mode resonance grating structures. We assess their performance optically, a method rarely reported, to investigate the device functionality and make practical comparisons to electron-beam lithography. We achieve a representative resolution of 30 nm, which leads to good optical resonances, but we also note issues with inconsistent patterning over large areas ($> 1\ \mathrm{mm}^2$) and short shelf-lives of the chemicals involved. We conclude that, while Nanoimprint lithography can fabricate structures on a par with electron beam lithography, it also presents some challenges in producing functional devices at lower throughputs, a key consideration for small research laboratories.

1. Introduction

Nanometre-scale optical structures underpin many applications and fuel much related research effort, e.g. in quantum photonics, optical communications, photonic sensing and augmented reality glasses, to name but a few areas. The natural choice for the fabrication of such structures is electron beam lithography (EBL), as it offers optimal precision and has become a mature technology. Nevertheless, EBL is slow, expensive and not necessarily accessible for a small research laboratory [1–3].

Nanoimprint lithography (NIL) promises a low-cost, high-throughput, high-resolution alternative, whereby imprint stamps are used to mechanically mould photoresist into nanostructure patterns, which, in principle, is independent of the size of the patterned area. Here, we examine a method of performing NIL with ultraviolet (UV) exposure (UV-NIL), as it is preferred over thermally cured NIL methods for achieving high-resolution patterning [4–7]. We assess the method by fabricating guided mode resonance (GMR) grating structures and validate the quality of the structures via their optical performance.

Such structures typically exhibit moderate resonance quality factors (Q-factors) of order $Q \approx 1e^2 - 1e^3$, and they require high structural consistency due to the extended nature of the resonant mode. The measured Q-factor and consistency of patterning over a large area are therefore key criteria for assessing the quality of the method, and we compare our results with the typical performance of structures made by electron-beam lithography, to determine if low throughput laboratories can benefit from the improved throughput of NIL when fabricating functional devices.

© 2026 The Author(s). Published by IOP Publishing Ltd

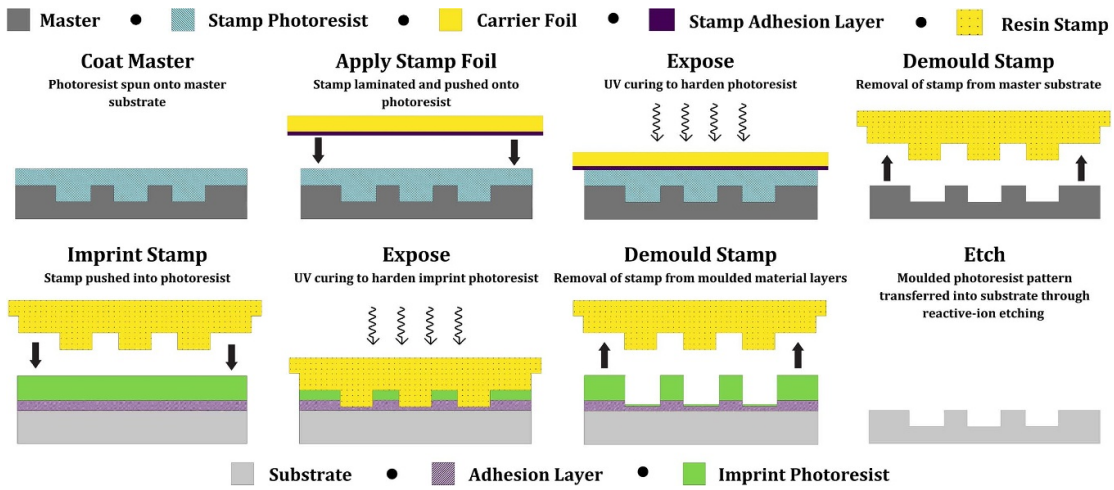

Figure 1. Schematic of the UV-NIL process outlining the production of the resin stamp, through application of GMN-PS380 and carrier foil, UV-exposure, the moulding and UV-exposure of the imprint photoresist material layer, and the final pattern transfer into the substrate through reactive-ion etching.

2. Materials and protocols

Our UV-NIL process is conducted on a CNI v3.0 NIL tool with a suite of chemicals from OpTool AB (Sweden) and Micro Resist Technology GmbH (Germany). The recently developed carrier foil, together with the GMN-PS380 stamp photoresist (OpTool AB), achieves enhancements in speed and simplicity for the creation of imprint stamps compared to the industry standard [8–10]. The new imprint stamps do not require thermal or anti-sticking treatment, and have been reported to achieve a feature size of 30 nm [5].

The following nomenclature will be used throughout this description: (1) Master: the initial patterned surface generated by EBL, (2) Carrier Foil: the flexible carrier component of the resin stamp, coated in OP-APEX adhesion promoter, (3) Resin Stamp: the cured GMN-PS380, used to copy the master, adhered to the carrier foil, (4) Substrate: the material to be patterned, and (5) Transfer: the resulting lithographically patterned sample. The process is summarized in figure 1.

2.1. Resin stamp protocol

We begin by cleaning the Master in a 3:1 sulfuric acid and hydrogen peroxide (Piranha) solution for 10 min. The Master is then spin-coated with the GMN-PS380 photoresist at 2000 rpm for 30 s. The carrier foil, which is pre-coated with an adhesion promoter (OpTool OP-APMEX) by the manufacturer, is then gently applied by hand, dropping from just above the photoresist layer, ensuring that the foil is larger than the sample to aid removal.

Next, we create the resin stamp by applying 1.2 bar to this sandwich for 6 s, using the CNI v3.0 NIL tool. This pressure ensures penetration of the resin stamp into the master's surface morphology. Without removal from the patterning tool, we then perform a UV exposure for 1 min to cure the polymer material, with an intensity of 50 mWcm^{-2}. Post-exposure, the resin stamp is removed from the Master using tweezers, delaminating the stamp in a direction parallel to the gratings.

This protocol produces large-area, high-fidelity resin stamps, with a spatial resolution of 30 nm as shown in figure 2, which is comparable to the resolution values quoted by others [5].

2.2. Imprint protocol

Substrates were cleaned using acetone and isopropanol, followed by oxygen plasma ashing to improve the surface adhesion. A further adhesion-promoting primer (Micro Resist mr-ADPROM) was applied via spin coating at 5000 rpm for 30 s and baked at 80 °C for 3 min. We used the imprint photoresist mr-NIL213FC (Micro Resist) and applied it via spin coating at 4000 rpm for 30 s, then baked it at 90 °C for 3 min. The resin stamp was applied to this substrate by hand, and the pattern transfer was completed in the CNI v3.0 NIL tool using 2 bar pressure for 1 min, followed by a 50 mW cm^{-2} UV exposure for 1 min when using silicon substrates. The exposure intensity was adjusted to 37.5 mW cm^{-2} when using silicon

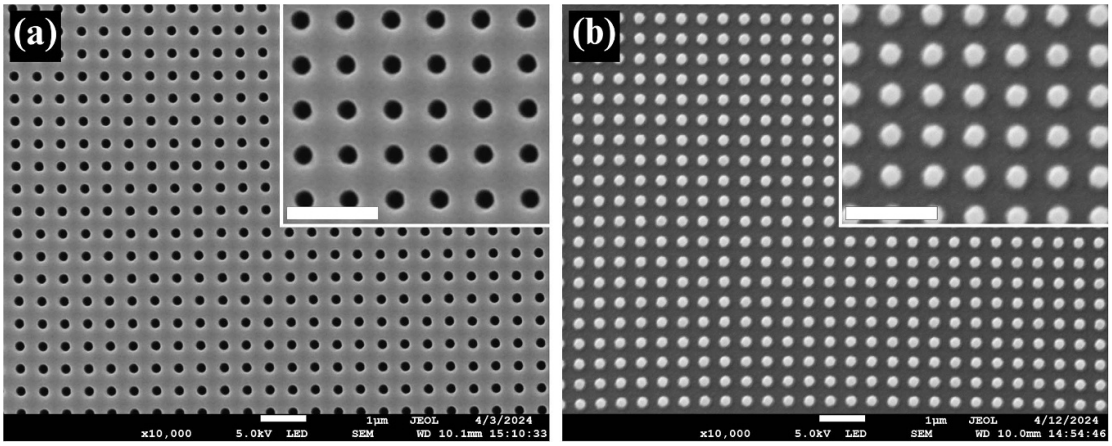

Figure 2. Scanning electron micrographs showing (a) a silicon master and (b) its negative copy as a resin stamp, demonstrating the high-fidelity inverse master replication. The scale bars represent 1 μm, and circular features are 215 nm in diameter.

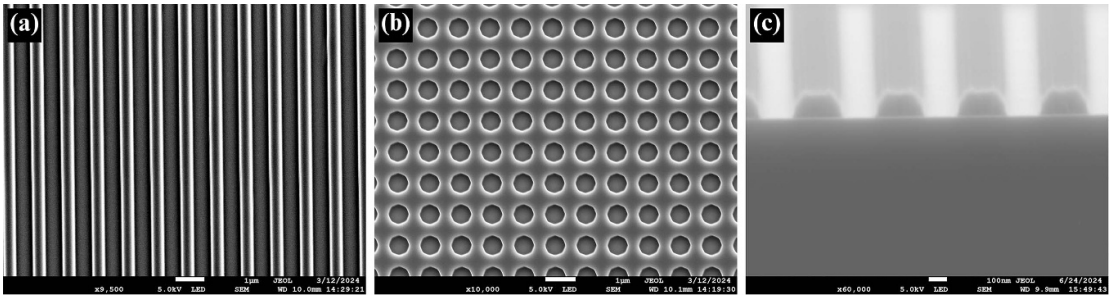

Figure 3. Scanning electron micrographs of a successful high-resolution transfer of a (a) one-dimensional and (b) two-dimensional grating, and (c) successful removal of the residual layer by reactive ion etching.

nitride substrates, accounting for its differing UV absorption. The resin stamp was finally removed, similarly to the stamp protocol. We optimized the complete parameter space to confirm this protocol, and identify transfer pressure as the most sensitive to achieve successful patterning.

Nanoimprinting typically leaves a residual layer, which forms a pedestal of unstructured resin. Using the process above, we typically observe a residual layer of approximately 120 nm thickness. This layer can be removed by dry etching, whereby the issue is to etch sufficiently long to fully remove the pedestal and clear the ridges, but not too long to remove the pattern altogether. We achieved this task using two separate methods: (1) plasma ashing in an oxygen environment for 40 s, with a chamber pressure of 0.2 mbar and a DC power of 200 W, (2) RIE in an oxygen environment for 40 s, with a chamber pressure of 0.13 mbar and a DC power of 42 W. We note that both plasma ashing and RIE are acceptable techniques for the removal of the residual layer (figure 3(c)).

We successfully fabricated both one- and two-dimensional GMR gratings. Note the high resolution, which is evidenced by the clear presence of the original e-beam pattern, designed as an array of octagonal holes (figure 3(b)). The success of the residual layer removal and clearing of the ridges is shown using reactive ion etching (figure 3(c)). Similar results were achieved with plasma ashing, where process control is easier to achieve as it is less aggressive.

To further test the NIL resolution, we reduced the period and feature size of structures; the results are shown in figure 4. We were successful in replicating features down to 100 nm, with spacings as small as 30 nm, which exceeds the requirements for typical GMR gratings. At this point, it is obvious that we are approaching the resolution limit; the structural quality is beginning to suffer, and circular features start to vary in shape and size. The resolution is comparable to that achieved with thick ($>$ 100 nm) photoresist using EBL. In the case if EBL, the resolution is limited by electron scattering within the layer, which is required to achieve necessary etch depth; hence we did not attempt using patterns with higher

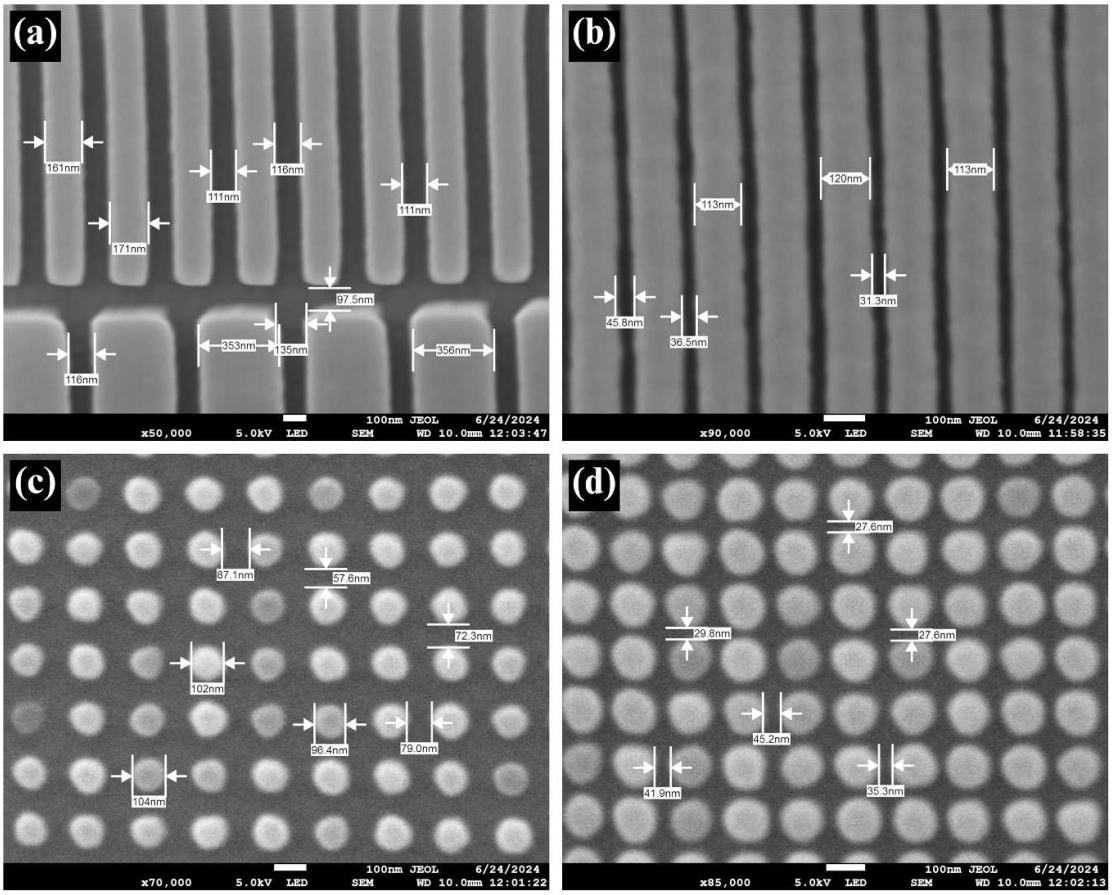

Figure 4. Scanning electron micrographs of (a)(b) one-dimensional and (c)(d) two-dimensional grating structures, highlighting feature size and spacing resolution limits achievable with the OpTool/Micro Resist NIL platform. The scale bars in all four micrographs represent 100 nm.

resolution. We note both NIL and EBL can indeed achieve higher resolution structures on thin resists, which however was not the purpose of our study as it does not afford the fabrication of functional grating structures.

2.3. Optical performance

So far, we have shown results that are commensurate with the literature, where researchers typically present high-quality structures with a focus on feature size. The added value we provide here is to highlight performance issues that are not apparent from the high-magnification SEM micrographs often presented, such as figures 2 and 3. In particular, we characterize the protocol and the fidelity of the produced pattern using the optical performance of the nanostructure, a method that is sensitive not only to the quality of the grating unit cell, but also to its larger-area uniformity.

We assessed a one-dimensional GMR grating, fabricated in a silicon nitride-coated borosilicate substrate, using a simple reflection setup illuminated using the collimated output of a halogen source. Comparison to the idealized performance simulated using rigorous coupled-wave analysis is also made. The results are shown in figure 5.

The performance of our grating is in broad agreement with the simulation. We adjusted the fill-factor and layer thickness within tolerances of the fabrication process to align the peak wavelength of the simulation to the measured value. The reduced amplitude in simulation (an ideal grating should have a resonance amplitude of unity) is explained by the asymmetry caused by the slight over etching ($\approx$ 10–20 nm) of the grating structure into the borosilicate substrate. The additional reduction in amplitude and Q-factor of the measured verses simulated resonance is most likely caused by roughness scattering; we typically observe a reduction in Q-factor between simulation and measurement by a factor of 1.5–2 for this reason, even in EBL-fabricated gratings, which suggests that the quality of the NIL grating is sufficient to support a good resonance.

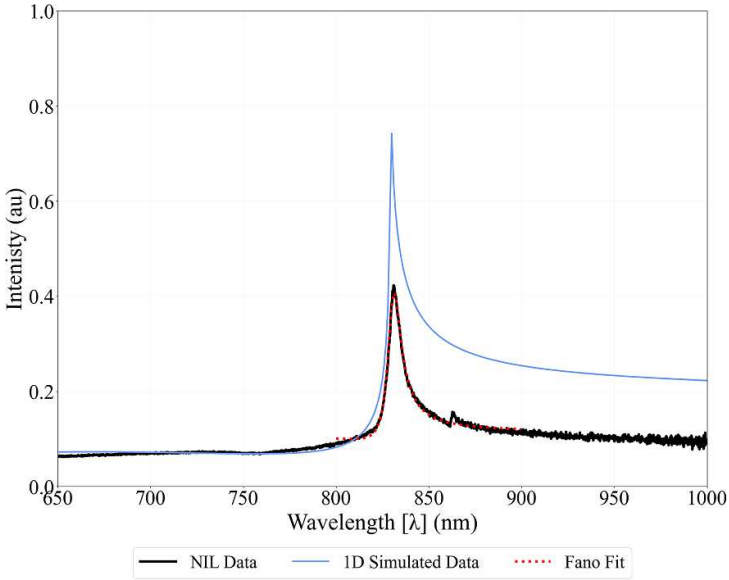

Figure 5. Experimentally measured resonance data, normalized to an aluminum mirror, in comparison to simulation. The data is taken for a 1D grating of 571 nm period and 75% fill factor, normalized to background, and fitting was completed using a Fano resonance. We observe a simulated Q-factor of $Q_{sim} = 160$, and an experimental Q-factor $Q_{exp} = 95$.

3. Protocol suitability

Having demonstrated the performance achievable with the OpTool-Micro Resist-NILT system, we will now consider some of the more practical aspects that are rarely mentioned in research papers. In particular, we consider patterning consistency over large areas as well as the limitations of the shelf-life of the relevant chemicals.

3.1. Large area consistency

Even though the nanoimprint process is, in principle, independent of area, we rarely managed to replicate patterns of millimetre size or larger, despite consistently applying the stamp and transfer protocols. We note that many papers in the literature highlight the ability to produce impressive high-resolution structures [5, 11–15]. However, functional devices often require larger area coverage, a requirement that we found difficult to replicate with this platform.

Peeling of the imprint photoresist (figure 6(a)) and incomplete patterning (figures 6(b)–(d) were consistent failures we encountered during patterning. It is difficult to quantify the average transferred area, though this consideration is immaterial as any value below 100% may render the device dysfunctional for a given application. Where patterns are replicated, they are replicated with high fidelity. While the small-area capability is clearly shown, such failings render the resonant structures less useful for practical applications. For example, only 1 in 15 samples was sufficiently complete to allow an optical measurement, as the one shown in figure 5, to be conducted. In contrast, large-area consistency is readily achieved by EBL with few/no errors, as demonstrated by our master fabrication and in the relevant literature [16–19].

We note that the imprint lithography process is adopted successfully in high-volume manufacturing processes, which use more expensive tools that achieve higher precision, as well as achieving much higher throughput, so the conclusions we present here do not apply.

3.2. Chemical lifetime

Assessment of the pattern fidelity as a function of chemical shelf life is critical when considering the requirements of a low throughput laboratory, as operating cost, namely consumables as these can be most directly compared, quickly accumulate where product is not exhausted before expiry.

We repeated the same experiments over a one-year timespan, and noticed a significant deterioration in replication quality after several months (M). The mr-ADPROM adhesion layers and mr-NIL-213FC imprint photoresist were delivered in February 2024 (M0), and the GMN-PS380 stamp photoresist was

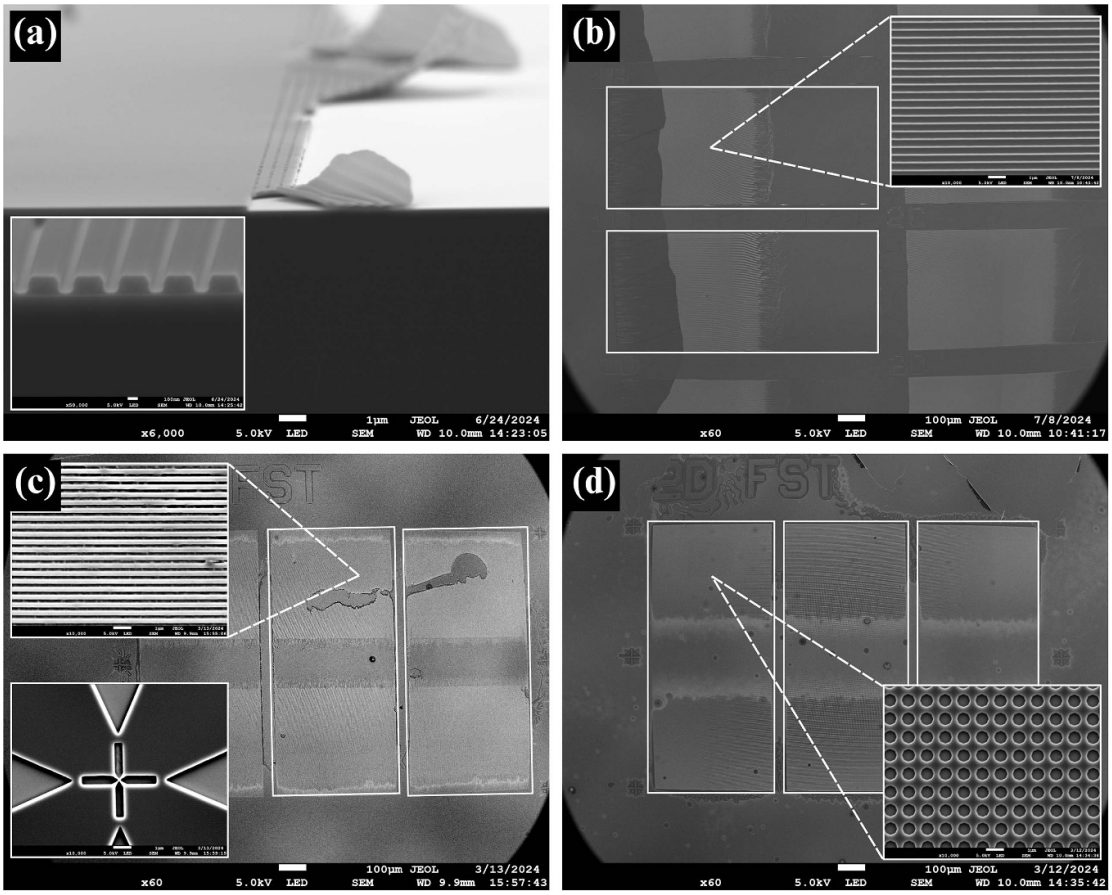

Figure 6. Scanning electron micrographs of large area pattern transfer, with inset regions of corresponding higher magnification micrographs. Such a comparison highlights the deception inherent in using small-area images to imply successful device fabrication. The white frames outline the regions where gratings were originally patterned but were only replicated in part.

delivered in M1, with respective expiries of M3, M5, and M7. Of these three chemicals, we realised that the adhesion layer was the critical chemistry, and Transfer using the old adhesive product failed irrespective of the freshness of the other chemistries; the Transfer quality recovered when using a new batch of mr-ADPROM. As it is difficult to quantify the pattern degradation as a function of shelf-life with any statistical relevance, we decided to highlight the phenomenon qualitatively and illustrate it in figure 7, in which Transfer quality post mr-ADPROM expiry (figure 7(c)) shows a severe decline.

In contrast, we note that the EBL photoresist we use (AR-P 6200.13 and AR-PC 5090 (Allresist)) can be used well beyond their official shelf-life. For example, we have been able to make the same high-quality structures with no apparent difference using the newly delivered resist, and 18 months post-delivery, 12 months after its expiry date. We note that a bottle of EBL resist costs approximately the same as the relevant NIL chemicals; in the same time as one EBL resist, one would need to buy approximately 5 bottles of mr-ADPROM adhesion layers, 2 bottles of mr-NIL-213FC imprint photoresist and 2 bottles of GMN-PS380 stamp photoresist, which yields a ratio of 9:1 in favor of EBL.

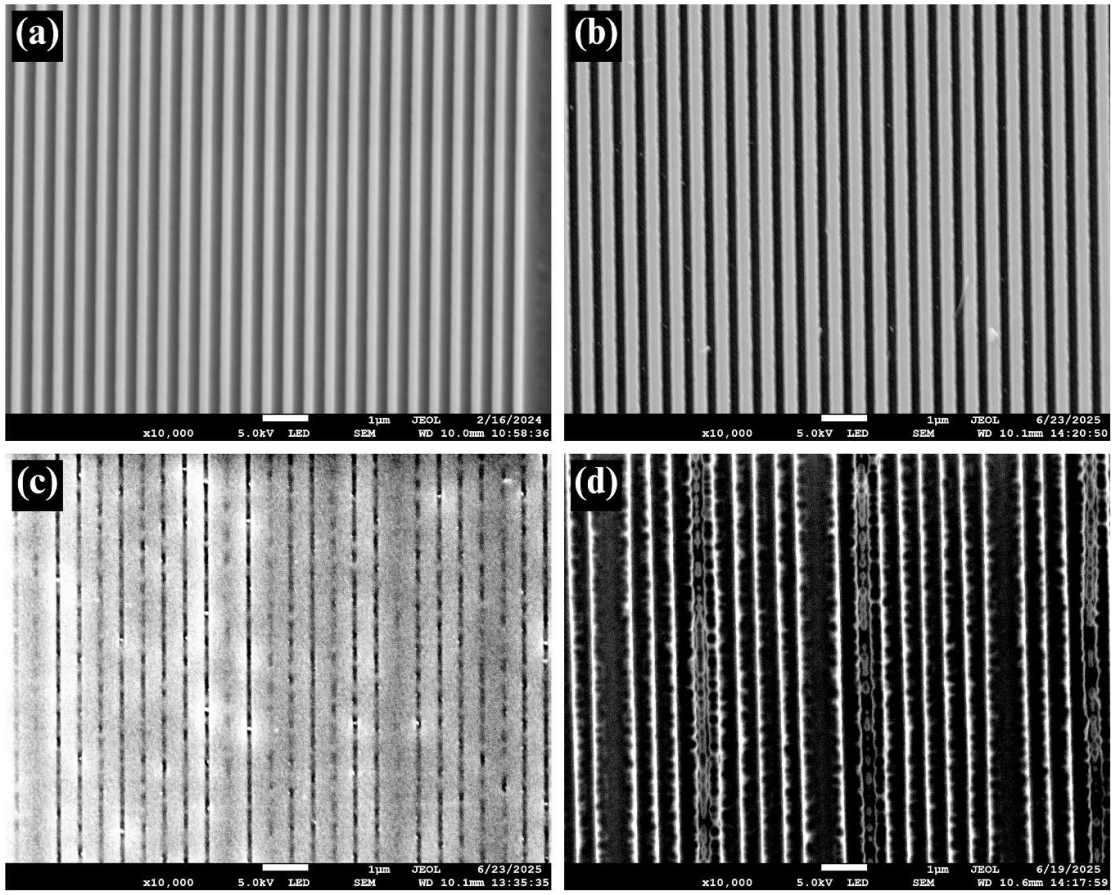

Figure 7. Scanning electron micrographs of structures fabricated as a function of time: (a) M0, (b) M2, (c) M4, and (d) M5. Significant deterioration in replication is visible from the expiry of the adhesion chemistry.

4. Conclusion

This work assesses the practical utility of UV-NIL, determining efficacy against its desirable criteria: low-cost, high-resolution, and high-fidelity substrate patterning. We used a new resin-stamp platform introduced by OpTool AB, and fabricated stamp patterns and GMR grating structures with comparable quality as reported in the literature. In addition, we evaluated pattern fidelity through optical characterisation, a method scarcely reported otherwise, yet essential for assessing the practical utility of the process in producing functional devices. We found that the resonance data agrees well with the simulation and that the ratio between simulated and experimental Q-factor is similar as observed for e-beam written gratings. On the other hand, we found that it was difficult to replicate large areas reliably i.e. much more difficult that what we typically experience with EBL. We also noted that some of the chemicals required for the NIL process had a very short shelf life, which severely limits their viability for a small-scale research laboratory, again, unlike our experience with EBL. Overall, while the OpTool NIL process is clearly capable of producing very high-quality structures, it does present some challenges for its use.

Acknowledgments

We acknowledge funding by UKRI through project EP/X037770/1. Further, the authors wish to acknowledge Dr Lisa Miller for her support and contributions to understanding the chemical interplay of material layers, and Dr Kezheng Li and Dr Pankaj Sahoo for their foundational work in the project.

Data availability statement

All data that support the findings of this study are included within the article. Raw data files can be provided upon request.

ORCID iDs

Timothy G Woodford 0009-0008-5362-7807
Joshua S Male 0000-0002-9579-3618
Christopher P Reardon 0000-0002-7550-6415
Thomas F Krauss 0000-0003-4367-6601

References

[1] Guo L J 2007 Nanoimprint lithography: methods and material requirements *Adv. Mater.* **19** 495–513
[2] Chen Y 2015 Nanofabrication by electron beam lithography and its applications *Microelectron. Eng.* **135** 57–72
[3] Ahn S H and Guo L J 2008 High-Speed Roll-to-Roll Nanoimprint Lithography on Flexible Plastic Substrates *Adv. Mater.* **20** 2044–9
[4] Colburn M *et al* 1999 Step and flash imprint lithography: a new approach to high-resolution patterning *Emerging Lithographic Technologies III* vol 3676 pp 379–89
[5] Asif M H, Graczyk M, Heidari B and Maximov I 2022 Comparison of UV-curable materials for high-resolution polymer nanoimprint stamps *Micro Nano Eng.* **14** 100118
[6] Suh D, Choi S-J and Lee H H 2005 Rigiflex lithography for nanostructure transfer *Adv. Mater.* **17** 1554–60
[7] Graczyk M, Cattoni A, Rösner B, Seniutinas G, Löfstrand A, Kvennefors A, Mailly D, David C and Maximov I 2018 Nanoimprint stamps with ultra-high resolution: optimal fabrication techniques *Microelectron. Eng.* **190** 73–78
[8] Carlberg P, Montelius L and Tegenfeldt J 2008 Nanoimprint in PDMS on glass with two-level hybrid stamp *Microelectron. Eng.* **85** 210–3
[9] Plachetka U, Bender M, Fuchs A, Vratzov B, Glinsner T, Lindner F and Kurz H 2004 Wafer scale patterning by soft UV-nanoimprint lithography *Microelectron. Eng.* **73-74** 167–71
[10] Tucher N, Höhn O, Hauser H, Müller C and Bläsi B 2017 Characterizing the degradation of PDMS stamps in nanoimprint lithography *Microelectron. Eng.* **180** 40–44
[11] Bossard M, Boussey J, Drogoff B L and Chaker M 2016 Alternative nano-structured thin-film materials used as durable thermal nanoimprint lithography templates *Nanotechnology* **27** 075302
[12] Barcelo S and Li. Z 2016 Nanoimprint lithography for nanodevice fabrication *Nano Converg.* **3** 21
[13] Schleunitz A, Guzenko V A, Messerschmidt M, Atasoy H, Kirchner R and Schift H 2014 Novel 3D micro- and nanofabrication method using thermally activated selective topography equilibration (TASTE) of polymers *Nano Converg.* **1** 7
[14] Wu W, Hu M, Ou F S, Li Z and Williams R S 2010 Cones fabricated by 3D nanoimprint lithography for highly sensitive surface enhanced Raman spectroscopy *Nanotechnology* **21** 255502
[15] Traub M C, Longsine W and Truskett V N 2016 Advances in nanoimprint lithography *Annu. Rev. Chem. Biomol. Eng.* **7** 583–604
[16] Sahoo P K, Coates E, Silver C D, Li K and Krauss T F 2024 On the reproducibility of electron-beam lithographic fabrication of photonic nanostructures *Sci. Rep.* **14** 8703
[17] Li K *et al* 2016 High speed e-beam writing for large area photonic nanostructures – a choice of parameters *Sci. Rep.* **6** 32945
[18] Martins A *et al* 2025 High efficiency glass-based VUV metasurfaces *Optica* **12** 1681–8
[19] Dey R K and Cui B 2013 Stitching error reduction in electron beam lithography with in-situ feedback using self-developing resist *J. Vac. Sci. Technol. B* **31** 06F409